AMERICAN
INSTITUTE OF
AERONAUTICS AND
ASTRONAUTICS

1290 AVENUE
OF THE AMERICAS
NEW YORK, N.Y. 10019
TELEPHONE
212 / 581-4300

November 9, 1973

To: Gifford A. Young

From: Ruth F. Bryans, Director, Scientific Publications

A back-up paper is enclosed for the following Synoptic:

Author(s): Fred Austin and George Zetkov

Title of Synoptic: Simulation Capability for Dynamics of Two-Body Flexible Satellites (Log No.A4844)

Title of Back-up Paper: same

Correspondence with: Mr. Fred Austin
Structural Mechanics Section
Grumman Aerospace Corporation
Bethpage, New York 11714

Journal: Journal of Spacecraft and Rockets

Scheduled Issue: March 1974

Ruth F. Bryans
(Miss) Ruth F. Bryans
by Teresa Heath

RFB:jg
Enc.

(NASA-CR-132375) SIMULATION CAPABILITY FOR DYNAMICS OF TWO-BODY FLEXIBLE SATELLITES (Grumman Aerospace Corp.) ~~18~~ 19 p HC $3.00 CSCL 14B

N74-12964

Unclas
G3/11 24566

SIMULATION CAPABILITY FOR DYNAMICS OF TWO-BODY FLEXIBLE SATELLITES

By

Fred Austin and George Zetkov

October 9, 1973

Backup Document for AIAA Synoptic Scheduled for
Publication in the Journal of Spacecraft and Rockets, March 1974

Structural Mechanics Section
Grumman Aerospace Corporation
Bethpage, New York 11714

SYNOPTIC BACKUP DOCUMENT

This document is made publicly available through the NASA scientific and technical information system as a service to readers of the corresponding "Synoptic" which is scheduled for publication in the following (checked) technical journal of the American Institute of Aeronautics and Astronautics.

- ☐ AIAA Journal
- ☐ Journal of Aircraft
- ☒ Journal of Spacecraft & Rockets, March 1974
- ☐ Journal of Hydronautics

A Synoptic is a brief journal article that presents the key results of an investigation in text, tabular, and graphical form. It is neither a long abstract nor a condensation of a full length paper, but is written by the authors with the specific purpose of presenting essential information in an easily assimilated manner. It is editorially and technically reviewed for publication just as is any manuscript submission. The author must, however, also submit a full backup paper to aid the editors and reviewers in their evaluation of the synoptic. The backup paper, which may be an original manuscript or a research report, is not required to conform to AIAA manuscript rules.

For the benefit of readers of the Synoptic who may wish to refer to this backup document, it is made available in this microfiche (or facsimile) form without editorial or makeup changes.

SIMULATION CAPABILITY FOR DYNAMICS OF TWO-BODY FLEXIBLE SATELLITES*

Fred Austin** and George Zetkov†
Grumman Aerospace Corporation
Bethpage, New York

Abstract

An analysis and computer program were prepared to realistically simulate the dynamic behavior of a class of satellites consisting of two end bodies separated by a connecting structure. The shape and mass distribution of the flexible end bodies are arbitrary; the connecting structure is flexible but massless and is capable of deployment and retraction. Fluid flowing in a piping system and rigid moving masses, representing a cargo elevator or crew members, have been modeled. Connecting Structure characteristics, control systems, and externally applied loads are modeled in easily replaced subroutines. Subroutines currently available include a telescopic beam-type connecting structure as well as attitude, deployment, spin, and wobble control. In addition, a unique mass balance control system was developed to sense and balance mass shifts due to the motion of a cargo elevator. The mass of the cargo may vary through a large range. Numerical results are discussed for various types of runs.

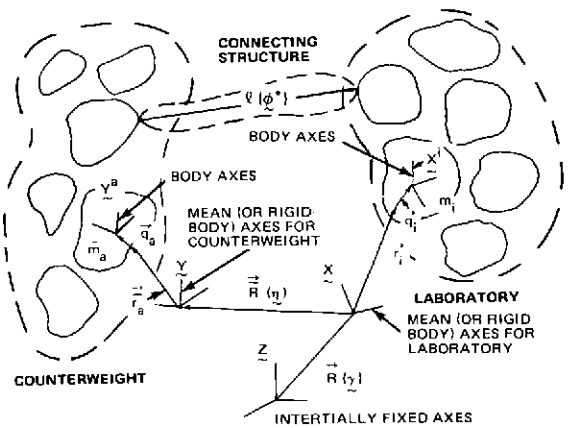

Fig. 1 Idealization and Coordinate Systems

I. Introduction

Often, when a new satellite configuration requires investigation, the equations of motion must be derived, programmed, and checked in order to predict the dynamic behavior of the vehicle. In this paper, a new computer program is described which eliminates these tasks for a class of two-body flexible satellites. One application is the rotating counterweight space station.

The end bodies are referred to herein as the Laboratory and the Counterweight, whereas the entire structure is referred to as the Space Station. The structure separating these bodies is referred to as the Connecting Structure. Both the Laboratory and the Counterweight are modeled as flexible structures with arbitrary shape and mass distribution (see Figure 1). The Connecting Structure is also flexible, but its mass is neglected.

Problems which may be studied using the program include deployment and retraction of the Connecting Structure with simultaneous or sequential spin-up and spin-down, the effects of moving rigid masses such as a cargo elevator or crew members on board the Laboratory, and the effect of fluid pumped through a piping system on the Laboratory. An example of a realistic configuration which may be treated is shown in Figure 2. Various features including control systems and Connecting Structure characteristics have been included in subroutine form so that these items may be easily replaced with minimum disruption to the main program. A subroutine is also provided for programming forces and torques; these may be applied at any mass point on the Space Station. Special constraint options permit the user to rigidize the entire Space Station or certain portions of the vehicle; thus the easier-understood rigid-body results can be compared with the more complex flexible-body solutions.

It is also possible to use the program to study the dynamics of the Laboratory alone when no Counterweight is present. Thus, many rotating and nonrotating satellite configurations can be studied since the Laboratory characteristics may be varied as input data.

---

*This work was performed for the NASA Langley Research Center under contract NAS 1-10973. The complete study is documented in References 1 and 2. Most of the content of this paper was presented at the AIAA Dynamics Specialist Conference at Williamsburg, Virginia on March 1973 (AIAA Paper No. 73-320, entitled "Simulation Capability for Dynamics of Rotating Counterweight Space Stations").

**Structural Mechanics Engineer

†Guidance and Control Engineer

The authors appreciate the technical and administrative assistance provided by Dr. R. Fralich, the NASA Project Monitor. Mr. S. Goldenberg performed all theoretical work required for the preprogram, which synthesizes the modes of the main structures. Dr. J. Markowitz's many significant technical contributions to this program are appreciated. Mr. E. Lowe programmed and checked both the main program and the preprogram, and his excellent work is gratefully acknowledged. Many of Mr. J. Smedfjeld's useful comments were incorporated into the manuscript.

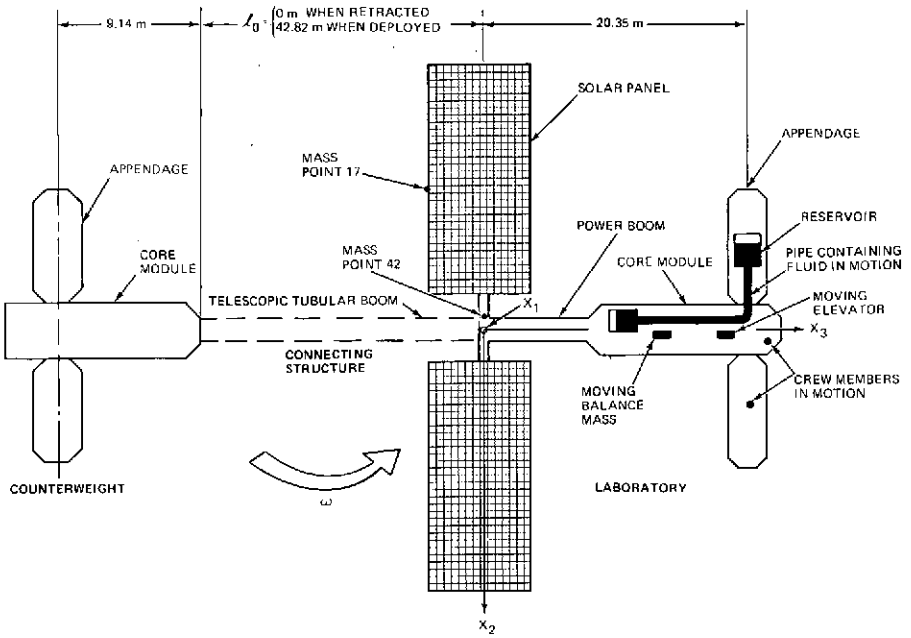

Fig. 2 Typical Configuration That Can Be Analyzed Using the Computer Program

II. Idealization and Method of Analysis*

The coordinates used in the analysis are shown in Figure 1. The $\underset{\sim}{X}$ axes are a system of mean axes moving with the average or "rigid-body" motion of the Laboratory and are used as the reference system for its elastic motion. Similarly, the $\underset{\sim}{Y}$ axes are a set of mean axes for the Counterweight. $\{R\}$ and the Euler angles $\{\gamma\}$ locate the $\underset{\sim}{X}$ axes in space, and $\{\bar{R}\}$ and $\{\eta\}$ locate the $\underset{\sim}{Y}$ axes with respect to the $\underset{\sim}{X}$ axes. The elastic linear and angular deflections with respect to the mean axes are $\{q_i\}$ and $\{\theta_i\}$, respectively, for a typical mass point m_i ($i = 1, \ldots, n$) on the Laboratory and $\{\bar{q}_a\}$ and $\{\bar{\theta}_a\}$ for a typical mass point $\bar{m}_a$ ($a = 1, \ldots, \bar{n}$) on the Counterweight. These elastic coordinates were linearized whenever there was an analytical or computational advantage to do so; however, the rigid-body coordinates $\{R\}$, $\{\gamma\}$, $\{\bar{R}\}$, and $\{\eta\}$ are not linearized so that large rigid-body motions may be studied. Instead of Euler-angle rates ($\{\dot{\gamma}\}$ and $\{\dot{\eta}\}$), angular velocities ($\{\omega^X\}$ and $\{\omega^Y\}$) of the $\underset{\sim}{X}$ and $\underset{\sim}{Y}$ axes, respectively, are used as integration coordinates in order to simplify the equations of motion. The angular-velocity components are not derivatives of generalized coordinates but are derivatives of quasi-coordinates. (3)

Newton and Euler equations of motion were written for an arbitrary number of lumped masses on the Laboratory and the Counterweight**, and the position and orientation of these masses is also arbitrary. The rotatory inertia of each structural mass point is included, as is linear and angular momentum of a fluid confined within a pipe segment on a typical Laboratory mass point. Any Laboratory mass points may also include the two fluid-system reservoirs; one is nominally filling and the other is nominally emptying. Uniform flow is assumed; thus slosh is not allowed. A maximum of eight moving rigid masses (a cargo elevator, crew motion, etc.) are idealized as point masses with no rotary inertia. Their rigid body motion is a prespecified function of time; however, the additional motion due to structural deformation of the path is estimated by averaging the motion of the surrounding structural masses and in this way is approximately included in the analysis.

The equations of motion were first written in vector form, and then converted to a convenient matrix form by using a set of identities developed for this purpose (see Appendix B of Reference 1). Next, modal or constraint relationships (or a combination of the two) were used to reduce the number of coordinates. For example, one type of constraint that may be selected by the program user is to rigidize the Laboratory or the Counterweight. After reduction of coordinates, the equations are linearly combined into a reduced number of equations by an automated technique described in Appendix D of Reference 1. The result is identical to that which would be obtained by writing Langrange's Equations for a system containing quasi-coordinates; however, the technique used in this analysis is more direct and simpler. The equations now have a symmetric acceleration coefficient matrix which was used to facilitate computation as follows. Because of nonlinear effects this matrix, and consequently its inverse, varies; therefore, the equations must be solved at each time point. Since more rapid computing algorithms are available for solving equations with symmetric coefficient matrices, the symmetric form led to appreciable time savings. Also, less storage is required since only the upper triangle of the matrix must be stored.

*Details of the analysis are presented in Reference 1.

**In the computer program the maximum number of lumped masses is 100 for each body.

When modes are used to represent the elastic motion of the Laboratory or Counterweight, a number of free-free elastic modes (but not rigid-body modes) of that structure are read into the program. Omitting the rigid-body modes uniquely determines the location of the $\underline{X}$ and $\underline{Y}$ mean axes of Figure 1 (see Section 4.3.5 of Reference 1). The modal masses and frequencies are required by the program and are used to define the stiffness characteristics of the structure; thus it is not required to read in a large physical stiffness matrix. Modal damping is assumed, and a different percentage of critical damping for each mode may be used.

III. Obtaining the Modes of Vibration

A separate preprogram was prepared to synthesize the modes of the Laboratory or Counterweight from a knowledge of the modes of their various component substructures. The synthesized modes may be passed directly from the preprogram to the main program.

To provide the versatility for synthesizing a wide variety of configurations, the procedure is developed for the general seventeen-module idealization shown in Figure 3. The user has the capability of eliminating any of the modules from this most general arrangement so long as he does not disconnect the structure. In this way, many configurations having a lesser number of flexible modules may be studied. The general configuration in Figure 3 allows up to five modules to be appended to one another in an arbitrary manner, and up to ten modules to be appended to one core module.

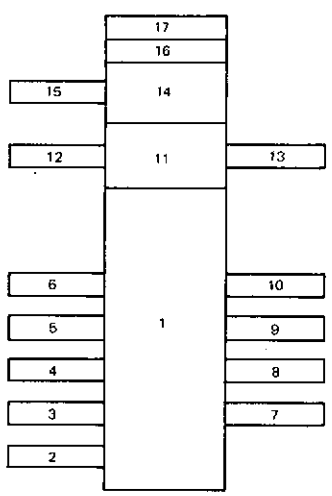

Fig. 3 General 17-Module Configuration for Modal Synthesis

One feature of the synthesis procedure is that the substructure modal matrices may be supplied in coordinate systems that are not parallel to the coordinate system in which the results, the coupled modes, are obtained. Accordingly, modules need not be in the same plane. In fact, they may be skewed at any angle in space.

Another feature of the procedure permits the user to supply constrained substructure modes. These are modes which were obtained for idealizations where constraints were employed; for example, in a beam analysis axial extension may have been neglected.

Capability is not provided to automatically synthesize structures where appendages are interconnected; however, modes for these structures may be obtained by other procedures and then used as input data to the main program. Thus, the main program is not restricted by the limitations of the preprogram.

IV. Control Systems

Five major types of control systems have been developed and programmed in subroutine form. The control and associated command subroutines were originally developed on a rigid-vehicle idealization and were then implemented on the flexible-vehicle computer program. Control actuators and sensors were assumed to move with the total motion of the mass point to which they were attached. The control systems are described briefly below.

Three-Axis Attitude-Position Control (when the vehicle is not spinning). Sixteen jets are mounted on the Laboratory for attitude-position control. The attitude error e and error rate $\dot{e}$ are measured about each axis, and the e and $\dot{e}$ combination is used to decide which jets to fire.

Spin Rate Control. The jets are also used for spin-up and spin-down maneuvers when these maneuvers are commanded by a spin command subroutine. In addition, these jets can be automatically fired to maintain a constant spin rate within a certain tolerance established by the control-system dead band.

Counterweight Position Control. This control system is used for deployment and retraction maneuvers. Unlike the other control systems, the actuator dynamics are not simulated. Rather, an idealized motor is assumed which is able to precisely control the undeformed length $\ell_0(t)$ of the connecting structure; i.e., $\ell_0(t)$ is set equal to a prespecified function of time contained in a position command subroutine. The input data to this subroutine are: the initial and final positions, the time for deployment to begin, the magnitude of an on-off constant acceleration $|\ddot{\ell}_0|$, and a maximum velocity $\dot{\ell}_{0\,max}$.

Wobble Control. A control moment gyroscope (CMG) is used to damp undesirable wobble due to gyroscopic effects when the vehicle is rotating. The highly efficient 90° h-lag law[4-7] is used to accomplish this task.

Mass Balancing for Spinning Vehicle. When the cargo elevator is in motion, the shifting of a large mass causes undesirable motions of the spinning vehicle. To balance this effect, an accelerometer detects the resulting accelerations, and a balance mass is moved to correct both the center of mass shift and the cross products of inertia of the vehicle.

Miscellaneous Command Subroutines. The same subroutine used to command the undeformed length of the Connecting Structure is also used to command the position (along each of the three axes) of every moving point mass except the balance mass (which is governed by the balance mass control system). There are a maximum of seven such moving masses which may be used to simulate the cargo elevator, crew members, etc. Another subroutine is used to prespecify the fluid velocity in the piping system, i.e., an idealized pump is assumed. Automatic shutoff occurs when a reservoir is either emptied or filled. This subroutine also generates the spin-rate command used as a reference input by the spin-rate control system.

V. Miscellaneous Program Capabilties

For reference, the program computes the position of the Space Station center of mass in inertial coordinates, the total angular momentum vector projected onto inertial coordinates, and the total system kinetic energy. The output includes $\{\delta\}$ and $\{\phi^*\}$, the linear and angular displacements, respectively, of the Connecting Structure attachment point on the Laboratory relative to the attachment point on the Counterweight. In addition, the program can compute the internal resultant force and torque vectors on any surface that separates the structure into two free bodies. This is accomplished by the acceleration method, which appears to be more accurate than the stiffness-damping matrix method for the case where a truncated number of modes represents the deformation of the vehicle.

VI. Program Checkout

Several test problems were run to check the program. In the test configuration, the Laboratory was idealized using eight structural masses and the Counterweight idealization had five structural masses. A telescopic boom was used as the Connecting Structure. First the entire vehicle was commanded to be rigid, and the time history was found to be identical to results obtained using the well-known analytical solutions for a rotating rigid body. Next, a separate program was written by an independent programmer using the theoretical expressions of Reference 1. However, this check program was much simpler than the main program since the expressions were applied only to the test configuration. Also, the time- and storage-saving manipulations used in the main program were not used in the test program. Several test runs were made, including vibration excited by: giving each variable and its derivative a different initial condition while rotating; fluid motion; point masses in motion; and a retraction maneuver. Time histories of the two programs agreed in each case.

The preprogram which synthesizes the modes of the Space Station was also tested by comparing results for several configurations with independently obtained results. The independent results were obtained by computing a mass and stiffness matrix for the entire structure by a standard technique and applying an existing eigenvalue program. Agreement was achieved in each case.

VII. Numerical Results Demonstrating the Computer Programs

Configuration. The NASA Langley Research Center provided Grumman with the configuration shown in Figure 2 for the purpose of demonstrating the computer program. The Laboratory is composed of a central core module with two relatively rigid appendages and two solar panels which are very flexible. The Connecting Structure is a telescopic beam which can be fully retracted. The Counterweight is composed of three relatively rigid modules. The mass of the entire vehicle is approximately 77,600 kg, and its deployed overall length is approximately 78.4 m. For additional descriptive details of this configuration see Reference 1.

First, the modes of the core and appended modules were computed by Grumman, based upon stiffness and mass properties generated by North American Rockwell. The modes of the solar panels were computed by Fairchild Industries and Wolf Research.[8] These modes were used as input data to the preprogram in order to obtain the free-free modes of the Laboratory and the Counterweight. The Counterweight was relatively rigid. The lowest flexible Counterweight frequency was 6.851 Hz, whereas the sixth Laboratory frequency was .382 Hz. It was therefore decided to idealize the Counterweight as a rigid body in the time-history computer program. The Laboratory was idealized using 72 mass points. Six flexible laboratory modes were then used to reduce the number of numerical-integration coordinates. Because of the relatively high flexibility of the solar panels, most of the motion in these modes is solar-panel motion. A total of 18 coordinates are used in the time-history runs. These are the six laboratory modes, six rigid-body coordinates locating the mean axes for the Laboratory, and six rigid-body coordinates for the Counterweight.

The connecting structure was assumed to be an elastic tubular beam with uniform characteristics per unit length. To approximate telescopic characteristics of the beam during deployment and retraction, new stiffness properties are computed at each time interval based on the beam length.

All control system jets, the CMG, and the control-system sensor package were mounted on the Laboratory core module.

A detailed description of the configuration is presented in Section 6.0 of Reference 1.

Selection of Runs. The runs which will be discussed are attitude control, deployment, spin-up, wobble control, elevator motion with mass balancing, and fluid being pumped between reservoirs. It is also possible to use the program to study many of these effects occurring simultaneously; however, this was not done in the present study. Since the runs performed were selected primarily to demonstrate the capability of the computer program, there was no attempt to optimize any of the operation parameters such as control-system gains. Also, in the case of the deployment and spin-up maneuvers, the jet thrusts were increased to unrealistic values in order to complete the maneuvers within 45 sec, thereby saving computer time.

Although the runs described herein are primarily flexible-vehicle runs, in each case the rigid-vehicle run was also performed. Rigidization was accomplished by using the program's constraint option.

Attitude Control. During the attitude-control maneuver, the system was not rotating and the Connecting Structure was fully retracted. The attitude control system developed for the rigid vehicle required no modification for use on the flexible-vehicle idealization. The three components of the Euler angles $\{\gamma\}$ orienting the vehicle are shown in Figure 4. Curves for a rigid-body run were overlayed with the flexible body curves of Figure 4 and no difference could be discerned. The Space Station was initially tilted so that each Euler angle was .01745 rad (1.0 deg). The control system then reduces each angle to the commanded value of zero. Similar behavior occurs along each of the three axes. The jets first apply a torque to begin correcting the attitude angle. Then a torque is applied in the negative direction to slow down the Space Station's angular rate. Linear deformation in the Connecting Structure is shown in Figure 5. Since the Connecting Structure is fully retracted, the illustrated deformation actually respesents the

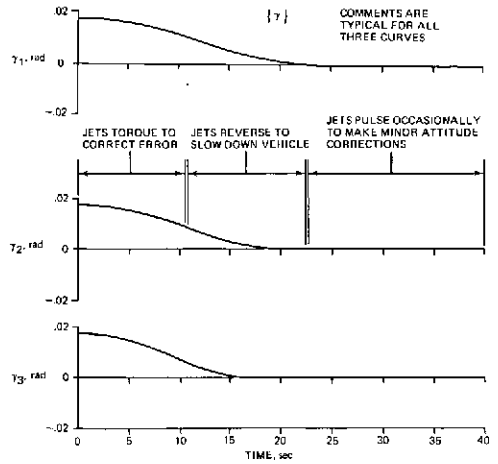

Fig. 4 Main-System Euler Angles $\{\gamma\}$ During Simultaneous Attitude Control Maneuver About All 3 Axes

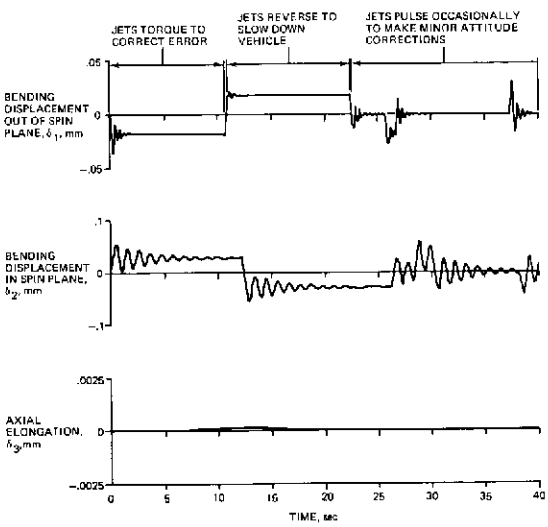

Fig. 5 Cantilever Deflection $\{\delta\}$ of Connecting Structure During Attitude Control Maneuver

very small deflections of the relatively stiff Connecting Structure docking hatch. This connection is only approximately represented as discussed in Section 4.4.2.1 of Reference 1.

Deployment with Spin-Rate Hold. Figure 6 illustrates a deployment maneuver at .2 rpm. All motion in this run is in the spin plane. Figure 6A shows the prespecified motion of the undeformed Connecting Structure. The Connecting Structure deploys from an undeformed length ℓ_{03} of 0 to 42.822 m. If the spin control system were not operational, the spin rate would decrease to maintain constant momentum; however, the command to maintain a constant spin rate was given during this run. To accomplish the deployment within 40 sec, the jet thrust was increased from a nominal value of 222.4 N (50 lb) to 4448.2 N (1000 lb). Figure 6B shows the axial deformation in the beam during deployment. Throughout the maneuver, the slow spin rate causes a slight centrifugal

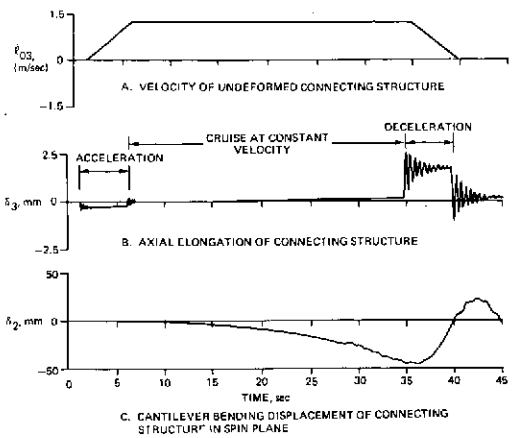

Fig. 6 Deployment Maneuver at .2 RPM

force. Therefore, there is a small tendency for the end bodies to separate naturally; however, this would occur at a very slow rate. The deployment command is given at t = 1 sec, and the Laboratory and the Counterweight are pushed apart ($\ddot{\ell}_{03} > 0$ as shown in Figure 6A) causing compression in the beam. When the maximum velocity $\dot{\ell}_{03}$ = 1.270 m/sec (50 in./sec) is reached, and deployment proceeds at constant velocity, the beam is expanded slightly by the centrifugal force. At approximately 35 sec, the deceleration begins ($\ddot{\ell}_{03} < 0$) and the expansion in the beam is increased significantly. Deployment ends at about 40 sec. The final expansion is much larger than the initial compression, mainly because the Connecting Structure is more flexible when more of it is deployed. For the same reason, the transient vibration occurs at a lower frequency when deployment is near completion. Figure 6C illustrates the bending of the Connecting Structure during deployment. This bending occurs partially as a result of the Coriolis forces, but primarily it is due to the spin jets torquing the Laboratory to maintain a constant angular velocity.

Spin-Up. Figures 7 and 8 illustrate a spin-up maneuver. The Space Station is initially rotating at .2 rpm and, at 5 sec, the command is given to increase the spin speed to 4 rpm. All motion in this run is in the spin plane. In order to accomplish the maneuver in 40 sec, the jets on the Laboratory were increased from 222.4 N (50 lb) to 66.7 kN (15,000 lb). Figure 7A illustrates the increase of the spin speed, and Figure 7B illustrates the corresponding increase in the axial extension of the Connecting Structure due primarily to the centrifugal force. Figure 7C shows the bending in the Connecting Structure during the spin-up maneuver. Unusually high bending deformations occur as a result of the large torques on the Laboratory generated by the increased jet thrusts. Figure 8 shows the largest component of the deformation at mass point 17, a very flexible point on a solar panel, and the largest component of the force exerted by the solar panel on the core module at the root of the panel (see Figure 2).

Quiescent State. When the Space Station is rotating in its nominal state of pure spin (i.e., in a state of pure rotation about the X_1 axis with no vibration), constant elastic deformations occur due to the centrifugal force. This state is known as the quiescent state. During the runs which were made when the

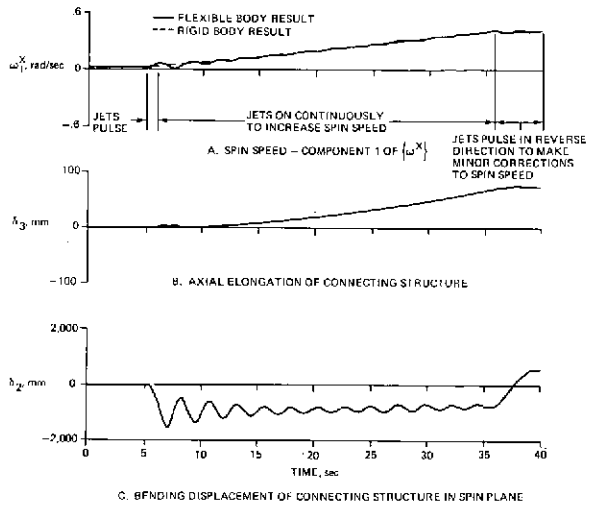

Fig. 7 Spin Speed and Cantilever Deflection of Connecting Structure During Spin-Up Maneuver

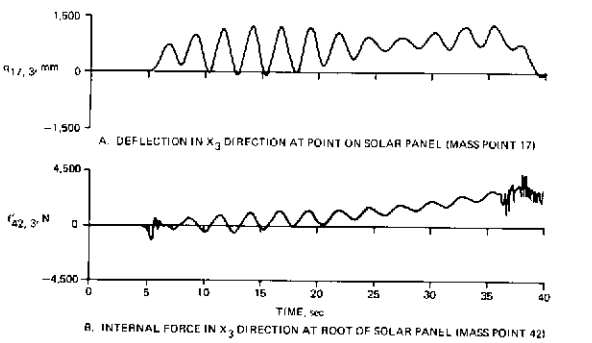

Fig. 8 Selected Deflection and Load Components During Spin-Up Maneuver

Space Station was rotating at its nominal spin speed of 4 rpm, the initial conditions are a variation from the quiescent state. Before making these runs, the quiescent state deformations were determined by setting all of the damping coefficients (for both the Laboratory and the Connecting Structure) to 80% of their critical values. A short run was made, and the deformations rapidly damped to their quiescent values. The quiescent deformations were highest at certain points on the solar panels. As an example, the deformation in the X_3 direction at mass point 17 ($q_{17,3}$) was approximately 540 mm (21.4 in.).

Wobble Control. Figure 9 illustrates the performance of the wobble control system. Initially, the deformations were set to their quiescent values, and the second component of $\{\omega^X\}$ was given a wobble component of .001 rad/sec. Up to approximately 27 sec the curves are essentially identical to a run made for a rigid Space Station. This indicates the usefulness of the mean axes; one reason that they were used was that they move at the average motion of the deformed system. After 27 sec, some small higher-frequency oscillations predominate due to elastic vibration. The only modification required to

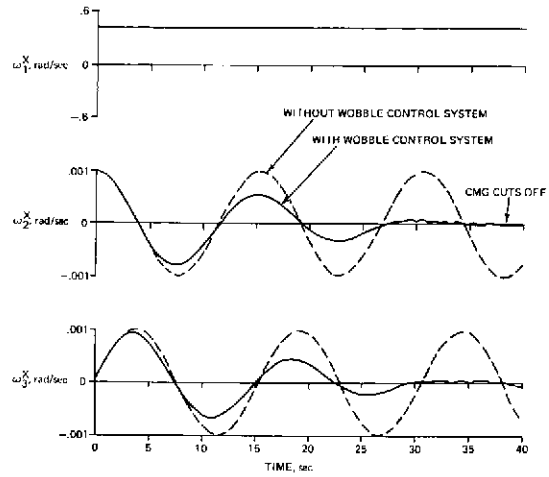

Fig. 9 Components of Angular Velocity $\{\omega^X\}$ Illustrating Wobble Control System

the CMG control system was to increase the amount of wobble at which the CMG stops trying to control wobble. Before this modification was made, the CMG sensor reacted to the residual vibration and the CMG continued to operate in the wobble-damping mode throughout the entire run.

Elevator Motion with Balance Mass Control. In the runs described in this paragraph, a 4,530 kg (10,000 lb) elevator and a 2,270 kg (5,000 lb) balance mass are initially located on the X_3 axis, at X_3=19.4 and 8.9 m, respectively. The elevator moves towards the balance mass at t=5 seconds. All rigid-body and flexible motion is in the spin plane. Initially, the Space Station is rotating in the quiescent state. The first balance-mass control system which was developed operated properly on a rigid-vehicle idealization; however, using the current computer program it was found that vehicle flexibility coupled undesirably with the control system. During this run the vehicle vibrated at a high-frequency vibration associated with the Connecting Structure axial mode, and the overall response of the balance mass was sluggish and unstable. The satisfactory control illustrated in Figure 10 was achieved after

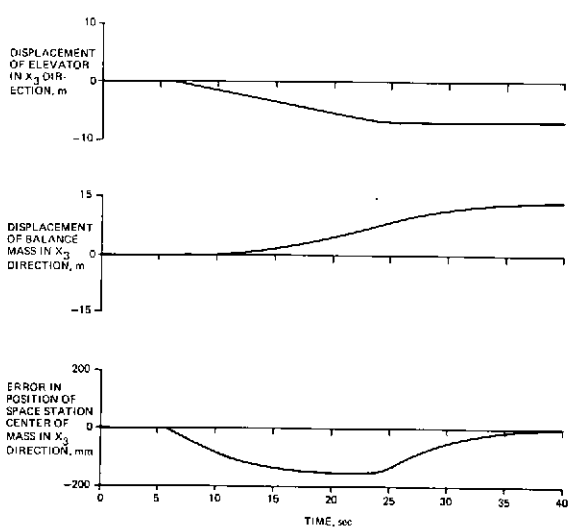

Fig. 10 Performance of Balance Mass Control System

considerable modification of the control law. The control system is required to balance an elevator motion of 7.00 m. The curve showing the error in the position of the Space Station center of mass indicates that there is a lag in the response of the balance mass; however, by the end of the run the Space Station is balanced. The deformations in the Connecting Structure during this run are shown in Figure 11. Note that there is an initial vibration although the elevator does not begin its motion until 5 sec. This initial vibration results because the initial quiescent deformations were obtained from a run where the elevator and balance masses were not present. The main Connecting-Structure bending effects are caused by the Coriolis forces exerted by the moving masses on the Laboratory and by the spin jets which torque the Laboratory to maintain the commanded constant spin speed. The deformation at mass point 17, which is on a solar panel, and the internal force exerted by the solar panel at its root are shown in Figures 12A and B.

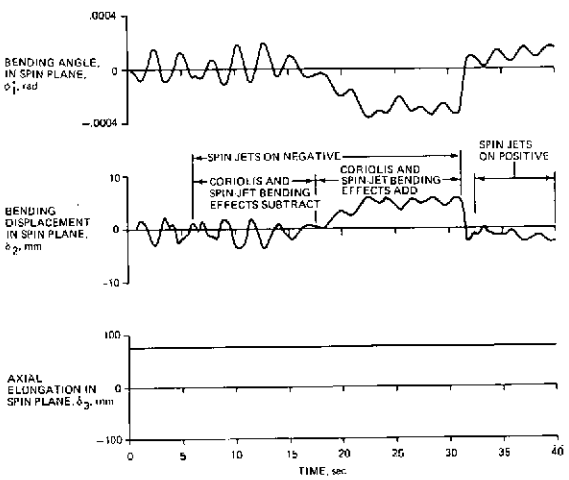

Fig. 11 Cantilever Deflection of Connecting Structure During Mass Balancing

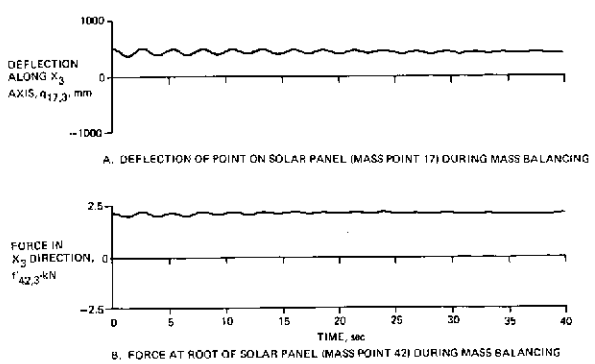

Fig. 12 Selected Deflection and Load Components During Mass Balancing

Fluid Pumped Through the Laboratory. In this run only, the Laboratory contained a fluid system consisting of a pipeline connecting two reservoirs. Unlike the system illustrated in Figure 2, the centerlines of both reservoirs and the pipe were located on the X_3 axis. Pumping begins at 2 sec. The fluid velocity and height of the fluid in the emptying reservoir are shown in Figure 13. Pumping proceeds until this reservoir is empty at t = 35.7 sec, when the pump suddenly shuts down. After shutdown, fluid remains in the pipeline. All motion during this run occurs in the spin plane. Figure 14 shows the deformations of the Connecting Structure. The bending which occurs during pumping is illustrated in Figure 15. The primary reason for this bending is that the resultant of the Coriolis forces exerted by the fluid acts to the left of the cm of the Laboratory as illustrated in the figure. This force also tends to slow the spin speed of the Laboratory slightly (from .4189 to .4149 rad/sec.). The control system is not present during this run; therefore, the spin jets do not turn on to correct the spin speed.

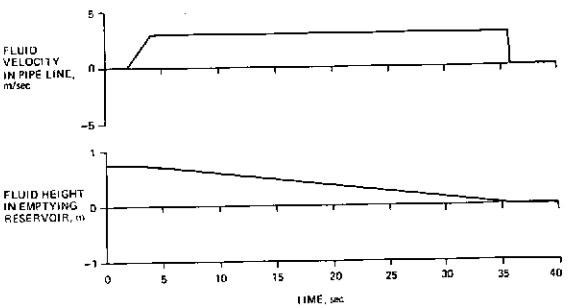

Fig. 13 Fluid Motion on the Laboratory

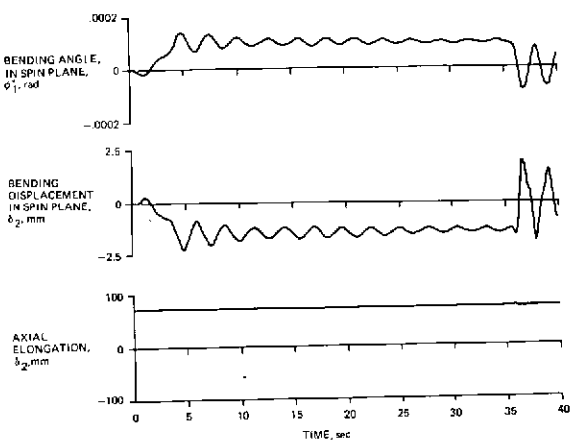

Fig. 14 Cantilever Deflection of Connecting Structure During Fluid Motion

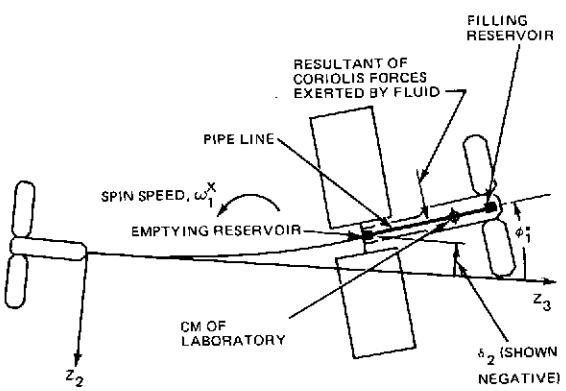

Fig. 15 Sketch Illustrating Bending (Exaggerated) in Connecting Structure During Fluid Motion

VIII. References

1. Austin, F., Markowitz, J., Goldenberg, S., and Zetkov, G., "A Study of the Dynamics of Rotating Space Stations with Elastically Connected Counterweight and Attached Flexible Appendages, Volume I, Theory, " NASA CR-112243, February 1973.

2. Lowe, E. and Austin, F., "A Study of the Dynamics of Rotating Space Stations with Elastically Connected Counterweight and Attached Flexible Appendages, Volume II, Computer Program User's Manual, " NASA CR-112244, February 1973.

3. Whittaker, E. T., "A Treatise on the Analytical Dynamics of Particles and Rigid Bodies," Fourth Edition, Cambridge University Press, 1937 (reprinted 1964), pp. 41-44.

4. Austin, F., and Berman, H., "Simple Approximations for Optimum Wobble Damping of Rotating Satellites Using a CMG," AIAA Journal, Vol. 10, No. 9, September 1972, pp. 1160-1164.

5. Austin, F. and Berman H., "Optimum Wobble Damping of Rotating Satellites Using a Control-Moment Gyroscope," Grumman Aerospace Corporation Report No. ADR 06-05-71.1, June 1971.

6. Berman H., Markowitz, J., and Holmer, W., "Study of Stability and Control Moment Gyro Wobble Damping of Flexible, Spinning Space Stations," Final Report, Prepared Under Contract NAS 9-11991 for the NASA Manned Spececraft Center by the Grumman Aerospace Corporation, February 1972; also AIAA Paper No. 72-888 presented at AIAA Guidance and Control Conference, August 1972.

7. Zetkov, G., Berman, H., Austin, F., Lidin, S., et al., "Study of Control Moment Gyroscope Applications to Space Base Wobble Damping and Attitude Control Systems," Grumman Guidance and Control Report No. GCR 70-4, September 1970; Prepared under Contract NAS 9-10427 for the NASA Manned Spacecraft Center by the Grumman Aerospace Corporation and the Sperry Flight Systems Division, September 1970.

8. Heindrichs, J. and Fee, J. "Integrated Dynamic Analysis Simulation of Space Stations With Controllable Solar Arrays (Supplemental Data and Analyses)" NASA CR-112145, September 1972.

SIMULATION CAPABILITY FOR DYNAMICS OF TWO-BODY FLEXIBLE SATELLITES*

Fred Austin** and George Zetkov†
Grumman Acrospace Corporation
Bethpage, New York

Abstract

An analysis and computer program were prepared to realistically simulate the dynamic behavior of a class of satellites consisting of two end bodies separated by a connecting structure. The shape and mass distribution of the flexible end bodies are arbitrary; the connecting structure is flexible but massless and is capable of deployment and retraction. Fluid flowing in a piping system and rigid moving masses, representing a cargo elevator or crew members, have been modeled. Connecting Structure characteristics, control systems, and externally applied loads are modeled in easily replaced subroutines. Subroutines currently available include a telescopic beam-type connecting structure as well as attitude, deployment, spin, and wobble control. In addition, a unique mass balance control system was developed to sense and balance mass shifts due to the motion of a cargo elevator. The mass of the cargo may vary through a large range. Numerical results are discussed for various types of runs.

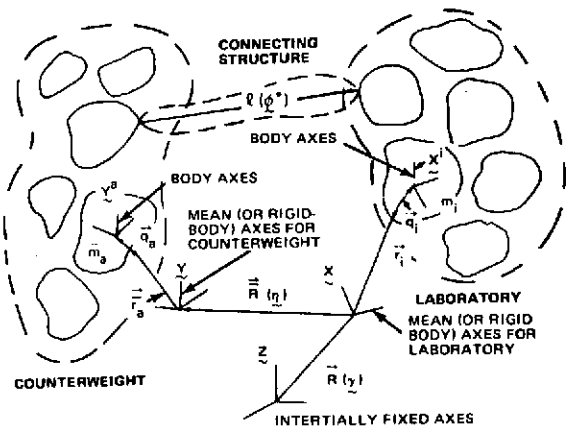

Fig. 1 Idealization and Coordinate Systems

1. Introduction

Often, when a new satellite configuration requires investigation, the equations of motion must be derived, programmed, and checked in order to predict the dynamic behavior of the vehicle. In this paper, a new computer program is described which eliminates these tasks for a class of two-body flexible satellites. One application is the rotating counterweight space station.

The end bodies are referred to herein as the Laboratory and the Counterweight, whereas the entire structure is referred to as the Space Station. The structure separating these bodies is referred to as the Connecting Structure. Both the Laboratory and the Counterweight are modeled as flexible structures with arbitrary shape and mass distribution (see Figure 1). The Connecting Structure is also flexible, but its mass is neglected.

Problems which may be studied using the program include deployment and retraction of the Connecting Structure with simultaneous or sequential spin-up and spin-down, the effects of moving rigid masses such as a cargo elevator or crew members on board the Laboratory, and the effect of fluid pumped through a piping system on the Laboratory. An example of a realistic configuration which may be treated is shown in Figure 2. Various features including control systems and Connecting Structure characteristics have been included in subroutine form so that these items may be easily replaced with minimum disruption to the main program. A subroutine is also provided for programming forces and torques; these may be applied at any mass point on the Space Station. Special constraint options permit the user to rigidize the entire Space Station or certain portions of the vehicle; thus the easier-understood rigid-body results can be compared with the more complex flexible-body solutions.

It is also possible to use the program to study the dynamics of the Laboratory alone when no Counterweight is present. Thus, many rotating and nonrotating satellite configurations can be studied since the Laboratory characteristics may be varied as input data.

---

*This work was performed for the NASA Langley Research Center under contract NAS 1-10973. The complete study is documented in References 1 and 2. Most of the content of this paper was presented at the AIAA Dynamics Specialist Conference at Williamsburg, Virginia on March 1973 (AIAA Paper No. 73-320, entitled "Simulation Capability for Dynamics of Rotating Counterweight Space Stations").

**Structural Mechanics Engineer

†Guidance and Control Engineer

The authors appreciate the technical and administrative assistance provided by Dr. R. Fralich, the NASA Project Monitor. Mr. S. Goldenberg performed all theoretical work required for the preprogram, which synthesizes the modes of the main structures. Dr. J. Markowitz's many significant technical contributions to this program are appreciated. Mr. E. Lowe programmed and checked both the main program and the preprogram, and his excellent work is gratefully acknowledged. Many of Mr. J. Smedfjeld's useful comments were incorporated into the manuscript.

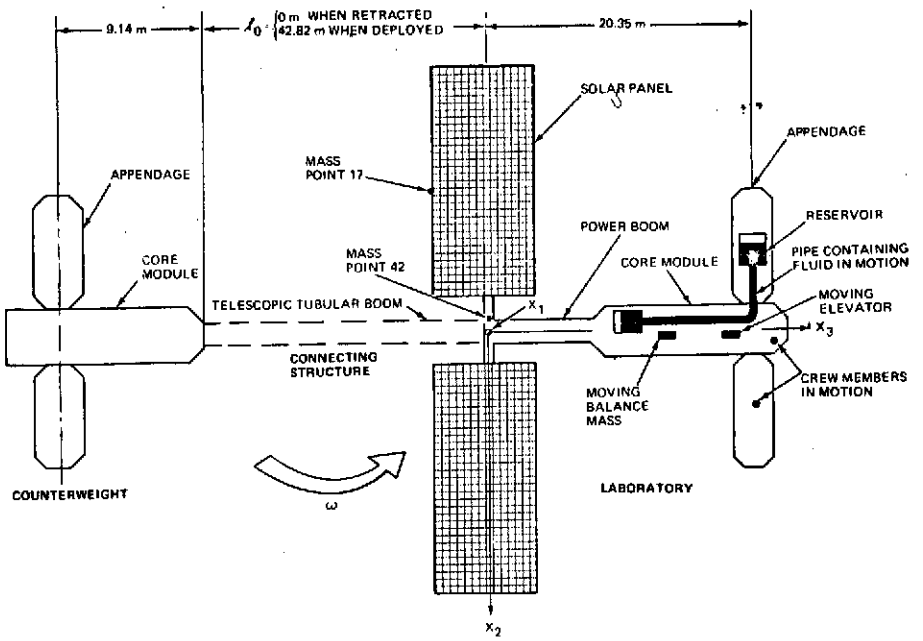

Fig. 2 Typical Configuration That Can Be Analyzed Using the Computer Program

II. Idealization and Method of Analysis*

The coordinates used in the analysis are shown in Figure 1. The $\underset{\sim}{X}$ axes are a system of mean axes moving with the average or "rigid-body" motion of the Laboratory and are used as the reference system for its elastic motion. Similarly, the $\underset{\sim}{Y}$ axes are a set of mean axes for the Counterweight. $\{R\}$ and the Euler angles $\{\gamma\}$ locate the $\underset{\sim}{X}$ axes in space, and $\{\bar{R}\}$ and $\{\eta\}$ locate the $\underset{\sim}{Y}$ axes with respect to the $\underset{\sim}{X}$ axes. The elastic linear and angular deflections with respect to the mean axes are $\{q_i\}$ and $\{\theta_i\}$, respectively, for a typical mass point m_i ($i = 1, \ldots, n$) on the Laboratory and $\{\bar{q}_a\}$ and $\{\bar{\theta}_a\}$ for a typical mass point $\bar{m}_a$ ($a = 1, \ldots, \bar{n}$) on the Counterweight. These elastic coordinates were linearized whenever there was an analytical or computational advantage to do so; however, the rigid-body coordinates $\{R\}$, $\{\gamma\}$, $\{\bar{R}\}$, and $\{\eta\}$ are not linearized so that large rigid-body motions may be studied. Instead of Euler angle rates ($\{\dot{\gamma}\}$ and $\{\dot{\eta}\}$), angular velocities ($\{\omega^X\}$ and $\{\omega^Y\}$) of the $\underset{\sim}{X}$ and $\underset{\sim}{Y}$ axes, respectively, are used as integration coordinates in order to simplify the equations of motion. The angular-velocity components are not derivatives of generalized coordinates but are derivatives of quasi-coordinates. (3)

Newton and Euler equations of motion were written for an arbitrary number of lumped masses on the Laboratory and the Counterweight**, and the position and orientation of these masses is also arbitrary. The rotatory inertia of each structural mass point is included, as is linear and angular momentum of a fluid confined within a pipe segment on a typical Laboratory mass point. Any Laboratory mass points may also include the two fluid-system reservoirs; one is nominally filling and the other is nominally emptying. Uniform flow is assumed; thus slosh is not allowed. A maximum of eight moving rigid masses (a cargo elevator, crew motion, etc.) are idealized as point masses with no rotary inertia. Their rigid body motion is a prespecified function of time; however, the additional motion due to structural deformation of the path is estimated by averaging the motion of the surrounding structural masses and in this way is approximately included in the analysis.

The equations of motion were first written in vector form, and then converted to a convenient matrix form by using a set of identities developed for this purpose (see Appendix B of Reference 1). Next, modal or constraint relationships (or a combination of the two) were used to reduce the number of coordinates. For example, one type of constraint that may be selected by the program user is to rigidize the Laboratory or the Counterweight. After reduction of coordinates, the equations are linearly combined into a reduced number of equations by an automated technique described in Appendix D of Reference 1. The result is identical to that which would be obtained by writing Langrange's Equations for a system containing quasi-coordinates; however, the technique used in this analysis is more direct and simpler. The equations now have a symmetric acceleration coefficient matrix which was used to facilitate computation as follows. Because of nonlinear effects this matrix, and consequently its inverse, varies; therefore, the equations must be solved at each time point. Since more rapid computing algorithms are available for solving equations with symmetric coefficient matrices, the symmetric form led to appreciable time savings. Also, less storage is required since only the upper triangle of the matrix must be stored.

*Details of the analysis are presented in Reference 1.

**In the computer program the maximum number of lumped masses is 100 for each body.

When modes are used to represent the elastic motion of the Laboratory or Counterweight, a number of free-free elastic modes (but not rigid-body modes) of that structure are read into the program. Omitting the rigid-body modes uniquely determines the location of the X and Y mean axes of Figure 1 (see Section 4.3.5 of Reference 1). The modal masses and frequencies are required by the program and are used to define the stiffness characteristics of the structure; thus it is not required to read in a large physical stiffness matrix. Modal damping is assumed, and a different percentage of critical damping for each mode may be used.

III. Obtaining the Modes of Vibration

A separate preprogram was prepared to synthesize the modes of the Laboratory or Counterweight from a knowledge of the modes of their various component substructures. The synthesized modes may be passed directly from the preprogram to the main program.

To provide the versatility for synthesizing a wide variety of configurations, the procedure is developed for the general seventeen-module idealization shown in Figure 3. The user has the capability of eliminating any of the modules from this most general arrangement so long as he does not disconnect the structure. In this way, many configurations having a lesser number of flexible modules may be studied. The general configuration in Figure 3 allows up to five modules to be appended to one another in an arbitrary manner, and up to ten modules to be appended to one core module.

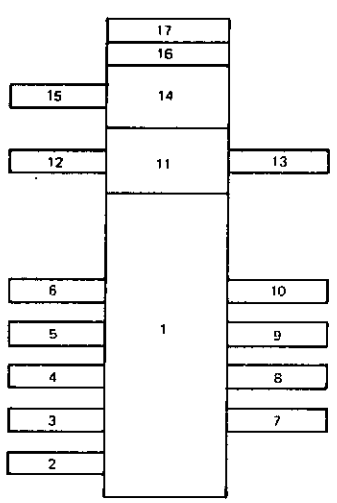

Fig. 3 General 17-Module Configuration for Modal Synthesis

One feature of the synthesis procedure is that the substructure modal matrices may be supplied in coordinate systems that are not parallel to the coordinate system in which the results, the coupled modes, are obtained. Accordingly, modules need not be in the same plane. In fact, they may be skewed at any angle in space.

Another feature of the procedure permits the user to supply constrained substructure modes. These are modes which were obtained for idealizations where constraints were employed; for example, in a beam analysis axial extension may have been neglected.

Capability is not provided to automatically synthesize structures where appendages are interconnected; however, modes for these structures may be obtained by other procedures and then used as input data to the main program. Thus, the main program is not restricted by the limitations of the preprogram.

IV. Control Systems

Five major types of control systems have been developed and programmed in subroutine form. The control and associated command subroutines were originally developed on a rigid-vehicle idealization and were then implemented on the flexible-vehicle computer program. Control actuators and sensors were assumed to move with the total motion of the mass point to which they were attached. The control systems are described briefly below.

Three-Axis Attitude-Position Control (when the vehicle is not spinning). Sixteen jets are mounted on the Laboratory for attitude-position control. The attitude error e and error rate $\dot{e}$ are measured about each axis, and the e and $\dot{e}$ combination is used to decide which jets to fire.

Spin Rate Control. The jets are also used for spin-up and spin-down maneuvers when these maneuvers are commanded by a spin command subroutine. In addition, these jets can be automatically fired to maintain a constant spin rate within a certain tolerance established by the control-system dead band.

Counterweight Position Control. This control system is used for deployment and retraction maneuvers. Unlike the other control systems, the actuator dynamics are not simulated. Rather, an idealized motor is assumed which is able to precisely control the undeformed length $\ell_0(t)$ of the connecting structure; i.e., $\ell_0(t)$ is set equal to a prespecified function of time contained in a position command subroutine. The input data to this subroutine are: the initial and final positions, the time for deployment to begin, the magnitude of an on-off constant acceleration $|\ddot{\ell}_0|$, and a maximum velocity $\dot{\ell}_{0\,\max}$.

Wobble Control. A control moment gyroscope (CMG) is used to damp undesirable wobble due to gyroscopic effects when the vehicle is rotating. The highly efficient 90° h-lag law[4-7] is used to accomplish this task.

Mass Balancing for Spinning Vehicle. When the cargo elevator is in motion, the shifting of a large mass causes undesirable motions of the spinning vehicle. To balance this effect, an accelerometer detects the resulting accelerations, and a balance mass is moved to correct both the center of mass shift and the cross products of inertia of the vehicle.

Miscellaneous Command Subroutines. The same subroutine used to command the undeformed length of the Connecting Structure is also used to command the position (along each of the three axes) of every moving point mass except the balance mass (which is governed by the balance mass control system). There are a maximum of seven such moving masses which may be used to simulate the cargo elevator, crew members, etc. Another subroutine is used to prespecify the fluid velocity in the piping system, i.e., an idealized pump is assumed. Automatic shutoff occurs when a reservoir is either emptied or filled. This subroutine also generates the spin-rate command used as a reference input by the spin-rate control system.

V. Miscellaneous Program Capabilties

For reference, the program computes the position of the Space Station center of mass in inertial coordinates, the total angular momentum vector projected onto inertial coordinates, and the total system kinetic energy. The output includes $\{\delta\}$ and $\{\phi^*\}$, the linear and angular displacements, respectively, of the Connecting Structure attachment point on the Laboratory relative to the attachment point on the Counterweight. In addition, the program can compute the internal resultant force and torque vectors on any surface that separates the structure into two free bodies. This is accomplished by the acceleration method, which appears to be more accurate than the stiffness-damping matrix method for the case where a truncated number of modes represents the deformation of the vehicle.

VI. Program Checkout

Several test problems were run to check the program. In the test configuration, the Laboratory was idealized using eight structural masses and the Counterweight idealization had five structural masses. A telescopic boom was used as the Connecting Structure. First the entire vehicle was commanded to be rigid, and the time history was found to be identical to results obtained using the well-known analytical solutions for a rotating rigid body. Next, a separate program was written by an independent programmer using the theoretical expressions of Reference 1. However, this check program was much simpler than the main program since the expressions were applied only to the test configuration. Also, the time- and storage-saving manipulations used in the main program were not used in the test program. Several test runs were made, including vibration excited by: giving each variable and its derivative a different initial condition while rotating; fluid motion; point masses in motion; and a retraction maneuver. Time histories of the two programs agreed in each case.

The preprogram which synthesizes the modes of the Space Station was also tested by comparing results for several configurations with independently obtained results. The independent results were obtained by computing a mass and stiffness matrix for the entire structure by a standard technique and applying an existing eigenvalue program. Agreement was achieved in each case.

VII. Numerical Results Demonstrating the Computer Programs

Configuration. The NASA Langley Research Center provided Grumman with the configuration shown in Figure 2 for the purpose of demonstrating the computer program. The Laboratory is composed of a central core module with two relatively rigid appendages and two solar panels which are very flexible. The Connecting Structure is a telescopic beam which can be fully retracted. The Counterweight is composed of three relatively rigid modules. The mass of the entire vehicle is approximately 77,600 kg, and its deployed overall length is approximately 78.4 m. For additional descriptive details of this configuration see Reference 1.

First, the modes of the core and appended modules were computed by Grumman, based upon stiffness and mass properties generated by North American Rockwell. The modes of the solar panels were computed by Fairchild Industries and Wolf Research.[8] These modes were used as input data to the preprogram in order to obtain the free-free modes of the Laboratory and the Counterweight. The Counterweight was relatively rigid. The lowest flexible Counterweight frequency was 6.851 Hz, whereas the sixth Laboratory frequency was .382 Hz. It was therefore decided to idealize the Counterweight as a rigid body in the time-history computer program. The Laboratory was idealized using 72 mass points. Six flexible laboratory modes were then used to reduce the number of numerical-integration coordinates. Because of the relatively high flexibility of the solar panels, most of the motion in these modes is solar-panel motion. A total of 18 coordinates are used in the time-history runs. These are the six laboratory modes, six rigid-body coordinates locating the mean axes for the Laboratory, and six rigid-body coordinates for the Counterweight.

The connecting structure was assumed to be an elastic tubular beam with uniform characteristics per unit length. To approximate telescopic characteristics of the beam during deployment and retraction, new stiffness properties are computed at each time interval based on the beam length.

All control system jets, the CMG, and the control-system sensor package were mounted on the Laboratory core module.

A detailed description of the configuration is presented in Section 6.0 of Reference 1.

Selection of Runs. The runs which will be discussed are attitude control, deployment, spin-up, wobble control, elevator motion with mass balancing, and fluid being pumped between reservoirs. It is also possible to use the program to study many of these effects occurring simultaneously; however, this was not done in the present study. Since the runs performed were selected primarily to demonstrate the capability of the computer program, there was no attempt to optimize any of the operation parameters such as control-system gains. Also, in the case of the deployment and spin-up maneuvers, the jet thrusts were increased to unrealistic values in order to complete the maneuvers within 45 sec, thereby saving computer time.

Although the runs described herein are primarily flexible-vehicle runs, in each case the rigid-vehicle run was also performed. Rigidization was accomplished by using the program's constraint option.

Attitude Control. During the attitude-control maneuver, the system was not rotating and the Connecting Structure was fully retracted. The attitude control system developed for the rigid vehicle required no modification for use on the flexible-vehicle idealization. The three components of the Euler angles $\{\gamma\}$ orienting the vehicle are shown in Figure 4. Curves for a rigid-body run were overlayed with the flexible body curves of Figure 4 and no difference could be discerned. The Space Station was initially tilted so that each Euler angle was .01745 rad (1.0 deg). The control system then reduces each angle to the commanded value of zero. Similar behavior occurs along each of the three axes. The jets first apply a torque to begin correcting the attitude angle. Then a torque is applied in the negative direction to slow down the Space Station's angular rate. Linear deformation in the Connecting Structure is shown in Figure 5. Since the Connecting Structure is fully retracted, the illustrated deformation actually respesents the

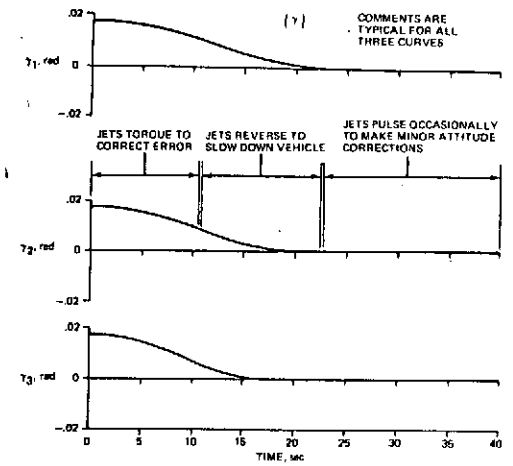

Fig. 4 Main-System Euler Angles $\{\gamma\}$ During Simultaneous Attitude Control Maneuver About All 3 Axes

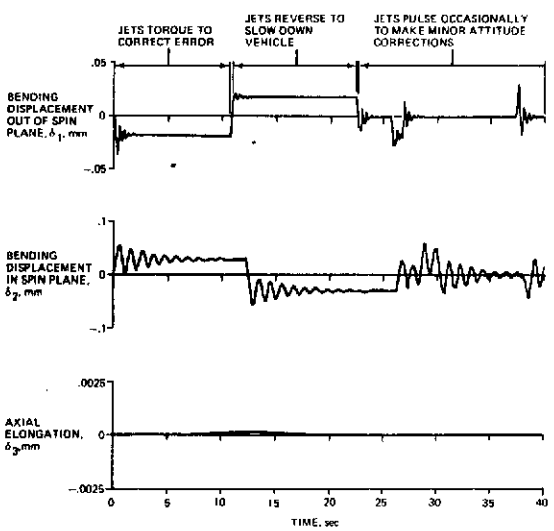

Fig. 5 Cantilever Deflection $\{\delta\}$ of Connecting Structure During Attitude Control Maneuver

very small deflections of the relatively stiff Connecting Structure docking hatch. This connection is only approximately represented as discussed in Section 4.4.2.1 of Reference 1.

Deployment with Spin-Rate Hold. Figure 6 illustrates a deployment maneuver at .2 rpm. All motion in this run is in the spin plane. Figure 6A shows the prespecified motion of the undeformed Connecting Structure. The Connecting Structure deploys from an undeformed length ℓ_{03} of 0 to 42.822 m. If the spin control system were not operational, the spin rate would decrease to maintain constant momentum; however, the command to maintain a constant spin rate was given during this run. To accomplish the deployment within 40 sec, the jet thrust was increased from a nominal value of 222.4 N (50 lb) to 4448.2 N (1000 lb). Figure 6B shows the axial deformation in the beam during deployment. Throughout the maneuver, the slow spin rate causes a slight centrifugal

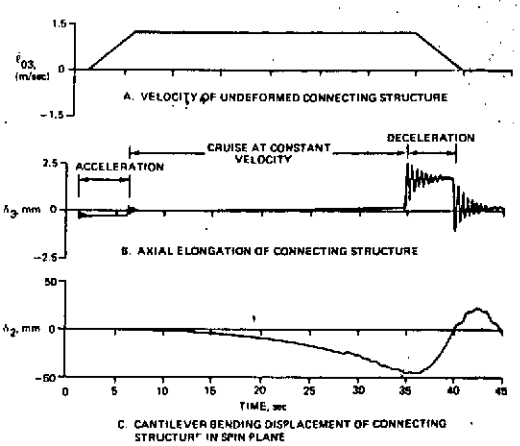

Fig. 6 Deployment Maneuver at .2 RPM

force. Therefore, there is a small tendency for the end bodies to separate naturally; however, this would occur at a very slow rate. The deployment command is given at t = 1 sec, and the Laboratory and the Counterweight are pushed apart ($\ddot{\ell}_{03} > 0$ as shown in Figure 6A) causing compression in the beam. When the maximum velocity $\dot{\ell}_{03} = 1.270$ m/sec (50 in./sec) is reached, and deployment proceeds at constant velocity, the beam is expanded slightly by the centrifugal force. At approximately 35 sec, the deceleration begins ($\ddot{\ell}_{03} < 0$) and the expansion in the beam is increased significantly. Deployment ends at about 40 sec. The final expansion is much larger than the initial compression, mainly because the Connecting Structure is more flexible when more of it is deployed. For the same reason, the transient vibration occurs at a lower frequency when deployment is near completion. Figure 6C illustrates the bending of the Connecting Structure during deployment. This bending occurs partially as a result of the Coriolis forces, but primarily it is due to the spin jets torquing the Laboratory to maintain a constant angular velocity.

Spin-Up. Figures 7 and 8 illustrate a spin-up maneuver. The Space Station is initially rotating at .2 rpm and, at 5 sec, the command is given to increase the spin speed to 4 rpm. All motion in this run is in the spin plane. In order to accomplish the maneuver in 40 sec, the jets on the Laboratory were increased from 222.4 N (50 lb) to 66.7 kN (15,000 lb). Figure 7A illustrates the increase of the spin speed, and Figure 7B illustrates the corresponding increase in the axial extension of the Connecting Structure due primarily to the centrifugal force. Figure 7C shows the bending in the Connecting Structure during the spin-up maneuver. Unusually high bending deformations occur as a result of the large torques on the Laboratory generated by the increased jet thrusts. Figure 8 shows the largest component of the deformation at mass point 17, a very flexible point on a solar panel, and the largest component of the force exerted by the solar panel on the core module at the root of the panel (see Figure 2).

Quiescent State. When the Space Station is rotating in its nominal state of pure spin (i.e., in a state of pure rotation about the X_1 axis with no vibration), constant elastic deformations occur due to the centrifugal force. This state is known as the quiescent state. During the runs which were made when the

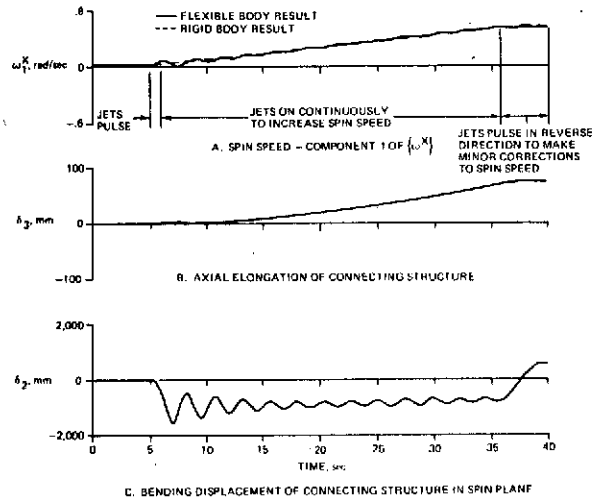

Fig. 7 Spin Speed and Cantilever Deflection of Connecting Structure During Spin-Up Maneuver

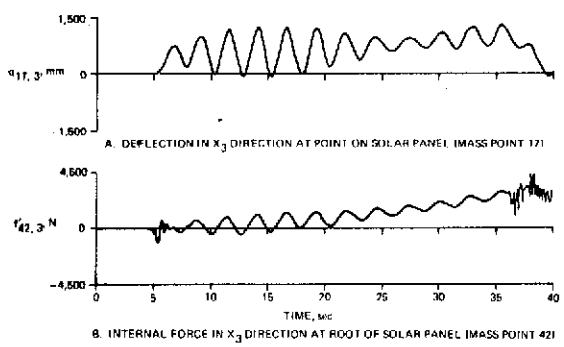

Fig. 8 Selected Deflection and Load Components During Spin-Up Maneuver

Space Station was rotating at its nominal spin speed of 4 rpm, the initial conditions are a variation from the quiescent state. Before making these runs, the quiescent state deformations were determined by setting all of the damping coefficients (for both the Laboratory and the Connecting Structure) to 80% of their critical values. A short run was made, and the deformations rapidly damped to their quiescent values. The quiescent deformations were highest at certain points on the solar panels. As an example, the deformation in the X_3 direction at mass point 17 ($q_{17,3}$) was approximately 540 mm (21.4 in.).

Wobble Control. Figure 9 illustrates the performance of the wobble control system. Initially, the deformations were set to their quiescent values, and the second component of $\{\omega^X\}$ was given a wobble component of .001 rad/sec. Up to approximately 27 sec the curves are essentially identical to a run made for a rigid Space Station. This indicates the usefulness of the mean axes; one reason that they were used was that they move at the average motion of the deformed system. After 27 sec, some small higher-frequency oscillations predominate due to elastic vibration. The only modification required to

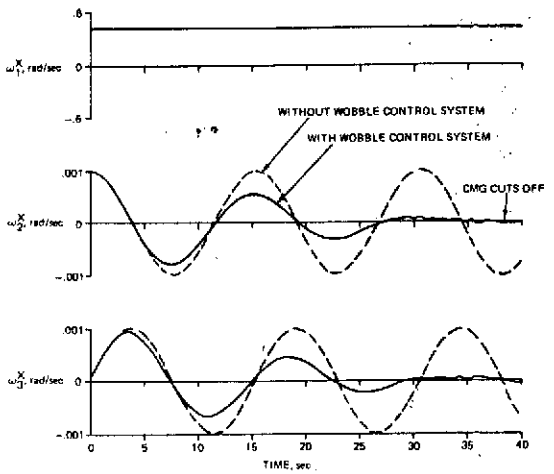

Fig. 9 Components of Angular Velocity $\{\omega^X\}$ Illustrating Wobble Control System

the CMG control system was to increase the amount of wobble at which the CMG stops trying to control wobble. Before this modification was made, the CMG sensor reacted to the residual vibration and the CMG continued to operate in the wobble-damping mode throughout the entire run.

Elevator Motion with Balance Mass Control. In the runs described in this paragraph, a 4,530 kg (10,000 lb) elevator and a 2,270 kg (5,000 lb) balance mass are initially located on the X_3 axis, at X_3=19.4 and 8.9 m, respectively. The elevator moves towards the balance mass at t=5 seconds. All rigid-body and flexible motion is in the spin plane. Initially, the Space Station is rotating in the quiescent state. The first balance-mass control system which was developed operated properly on a rigid-vehicle idealization; however, using the current computer program it was found that vehicle flexibility coupled undesirably with the control system. During this run the vehicle vibrated at a high-frequency vibration associated with the Connecting Structure axial mode, and the overall response of the balance mass was sluggish and unstable. The satisfactory control illustrated in Figure 10 was achieved after

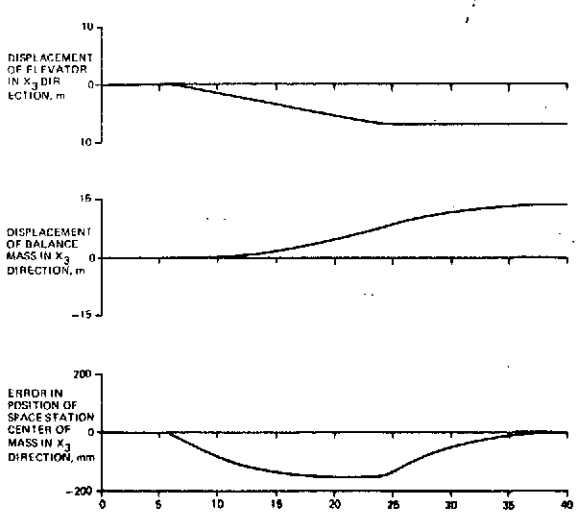

Fig. 10 Performance of Balance Mass Control System

considerable modification of the control law. The control system is required to balance an elevator motion of 7.00 m. The curve showing the error in the position of the Space Station center of mass indicates that there is a lag in the response of the balance mass; however, by the end of the run the Space Station is balanced. The deformations in the Connecting Structure during this run are shown in Figure 11. Note that there is an initial vibration although the elevator does not begin its motion until 5 sec. This initial vibration results because the initial quiescent deformations were obtained from a run where the elevator and balance masses were not present. The main Connecting-Structure bending effects are caused by the Coriolis forces exerted by the moving masses on the Laboratory and by the spin jets which torque the Laboratory to maintain the commanded constant spin speed. The deformation at mass point 17, which is on a solar panel, and the internal force exerted by the solar panel at its root are shown in Figures 12A and B.

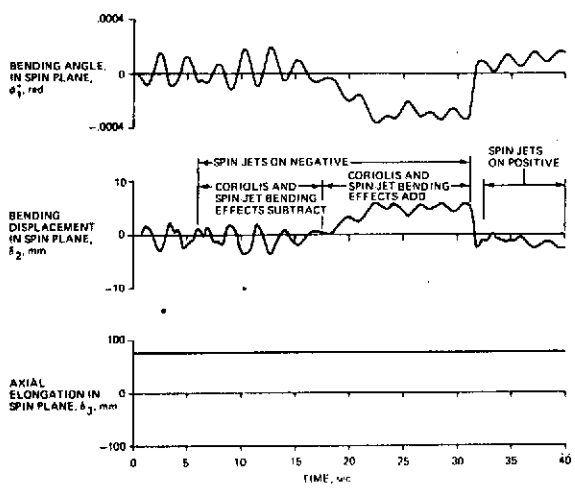

Fig. 11 Cantilever Deflection of Connecting Structure During Mass Balancing

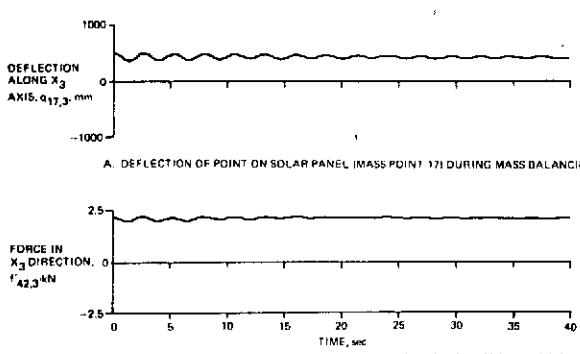

Fig. 12 Selected Deflection and Load Components During Mass Balancing

Fluid Pumped Through the Laboratory. In this run only, the Laboratory contained a fluid system consisting of a pipeline connecting two reservoirs. Unlike the system illustrated in Figure 2, the centerlines of both reservoirs and the pipe were located on the X_3 axis. Pumping begins at 2 sec. The fluid velocity and height of the fluid in the emptying reservoir are shown in Figure 13. Pumping proceeds until this reservoir is empty at t = 35.7 sec, when the pump suddenly shuts down. After shutdown, fluid remains in the pipeline. All motion during this run occurs in the spin plane. Figure 14 shows the deformations of the Connecting Structure. The bending which occurs during pumping is illustrated in Figure 15. The primary reason for this bending is that the resultant of the Coriolis forces exerted by the fluid acts to the left of the cm of the Laboratory as illustrated in the figure. This force also tends to slow the spin speed of the Laboratory slightly (from .4189 to .4149 rad/sec.). The control system is not present during this run; therefore, the spin jets do not turn on to correct the spin speed.

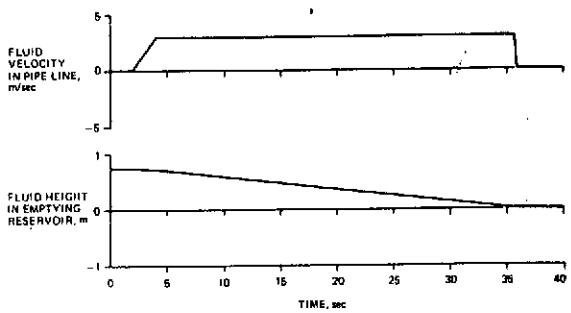

Fig. 13 Fluid Motion on the Laboratory

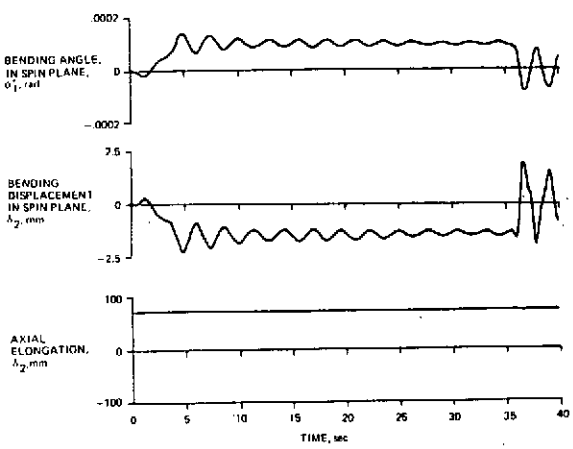

Fig. 14 Cantilever Deflection of Connecting Structure During Fluid Motion

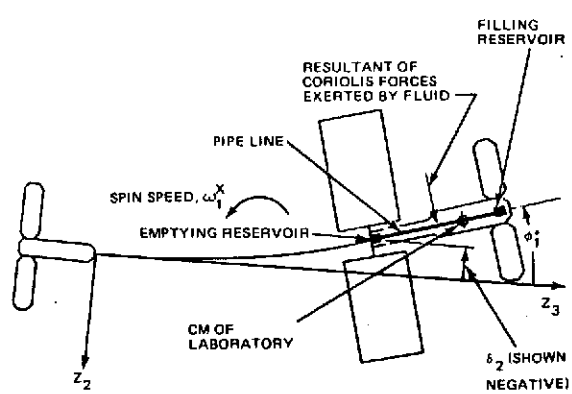

Fig. 15 Sketch Illustrating Bending (Exaggerated) in Connecting Structure During Fluid Motion

VIII. References

1. Austin, F., Markowitz, J., Goldenberg, S., nd Zetkov, G., "A Study of the Dynamics of Rotating ipace Stations with Elastically Connected Counter- veight and Attached Flexible Appendages, Volume I, heory, " NASA CR-112243, February 1973.

2. Lowe, E. and Austin, F., "A Study of the)ynamics of Rotating Space Stations with Elastically :onnected Counterweight and Attached Flexible ippendages, Volume II, Computer Program User's Manual, " NASA CR-112244, February 1973.

3. Whittaker, E. T., "A Treatise on the nalytical Dynamics of Particles and Rigid Bodies, " 'ourth Edition, Cambridge University Press, 1937 reprinted 1964), pp. 41-44.

4. Austin, F., and Berman, H., "Simple ipproximations for Optimum Wobble Damping of lotating Satellites Using a CMG, " AIAA Journal, 'ol. 10, No. 9, September 1972, pp. 1160-1164.

5. Austin, F. and Berman H., "Optimum Wobble)amping of Rotating Satellites Using a Control-Moment Gyroscope, " Grumman Aerospace Corporation Report No. ADR 06-05-71.1, June 1971.

6. Berman H., Markowitz, J., and Holmer, W., "Study of Stability and Control Moment Gyro Wobble Damping of Flexible, Spinning Space Stations, " Final Report, Prepared Under Contract NAS 9-11991 for the NASA Manned Spececraft Center by the Grumman Aerospace Corporation, February 1972; also AIAA Paper No. 72-888 presented at AIAA Guidance and Control Conference, August 1972.

7. Zetkov, G., Berman, H., Austin, F., Lidin, S., et al., "Study of Control Moment Gyroscope Applications to Space Base Wobble Damping and Attitude Control Systems, " Grumman Guidance and Control Report No. GCR 70-4, September 1970; Prepared under Contract NAS 9-10427 for the NASA Manned Spacecraft Center by the Grumman Aerospace Corporation and the Sperry Flight Systems Division, September 1970.

8. Heindrichs, J. and Fee, J. "Integrated Dynamic Analysis Simulation of Space Stations With Controllable Solar Arrays (Supplemental Data and Analyses)" NASA CR-112145, September 1972.